

# Delineation of High-Dip Structure at SAFOD using Drillnoise and Earthquake Data

D E Miller, S T Taylor,  
J Haldorsen, R. Coates

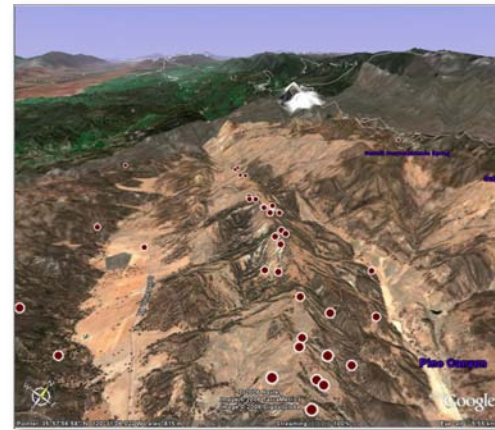
FISH seminar

Dec 3, 2010

# Outline

- SAFOD & the Duke/USGS Data set
- A Bit of Interferometry
- Simple Tomography with Earthquake Source Data

# San Andreas Fault Observatory at Depth (SAFOD)



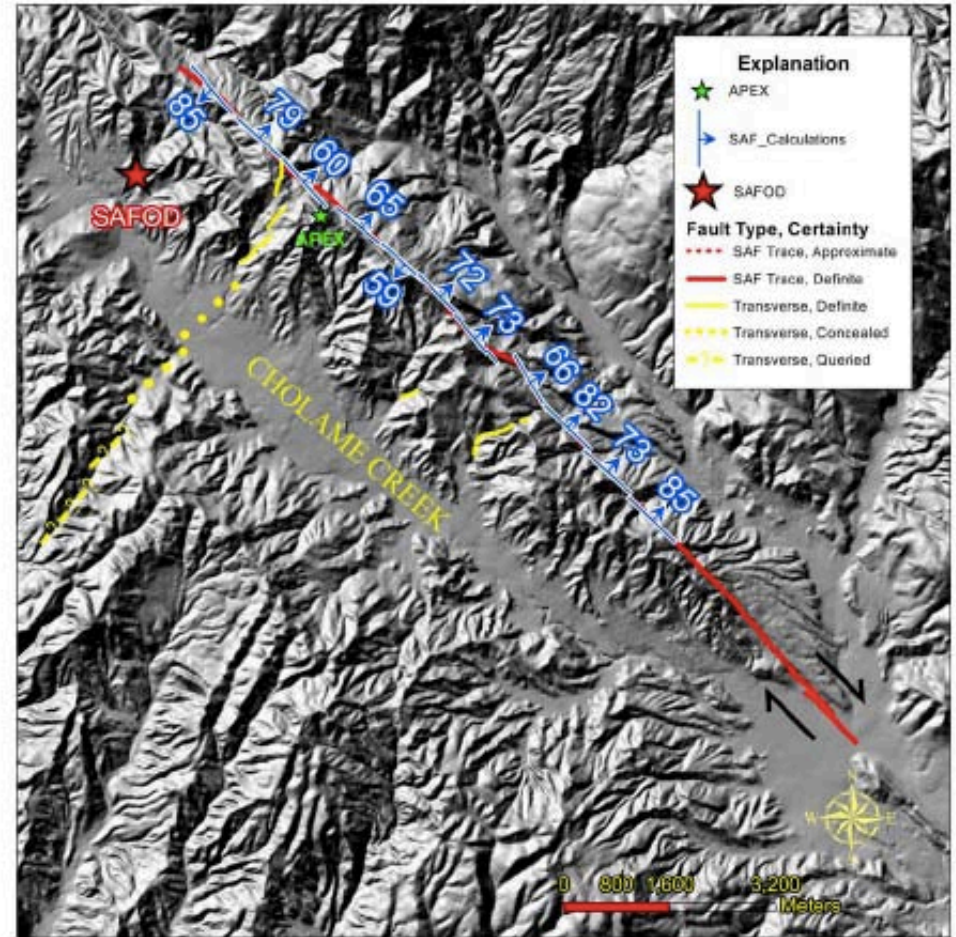
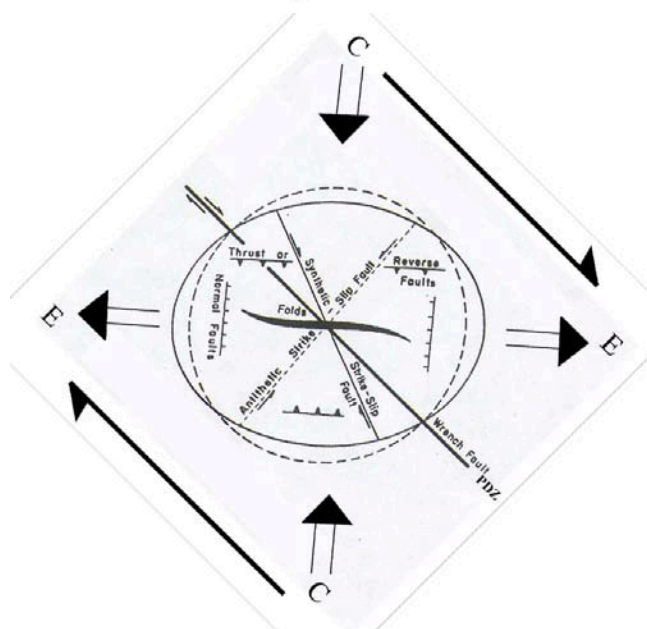
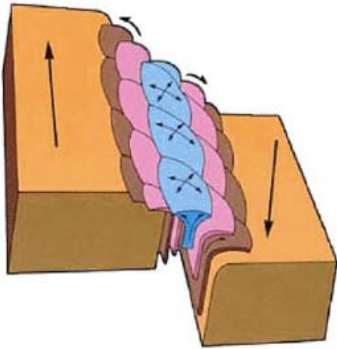
- Consortium of Universities and USGS
- SLB sold and contributed logs and DNVSP
- Tom Taylor acquired DNVSP as PhD project at Duke

STRUCTURAL GEOLOGY OF THE SAN ANDREAS FAULT ZONE AT MIDDLE MOUNTAIN, NEAR PARKFIELD, CENTRAL CALIFORNIA

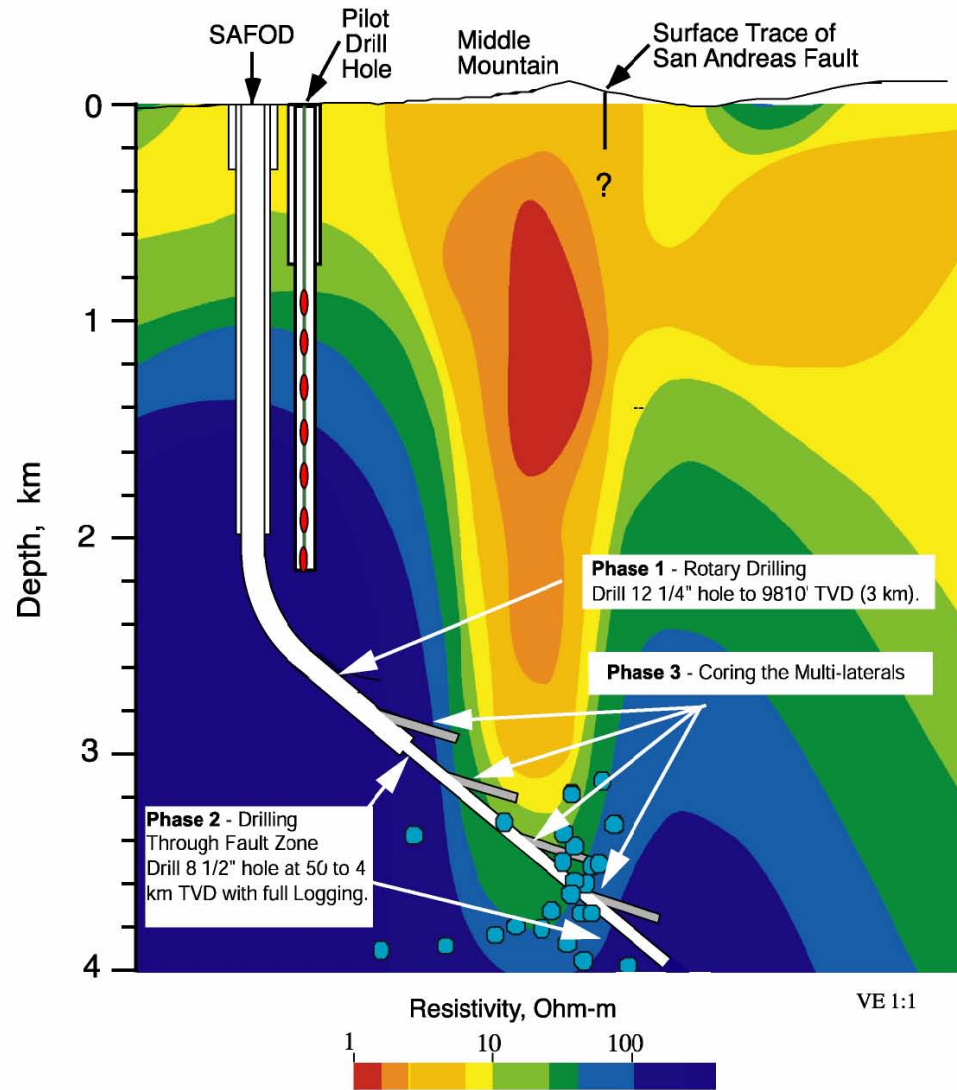
by  
Maurits Thayer

ARIZONA STATE UNIVERSITY

May 2006



# Plan

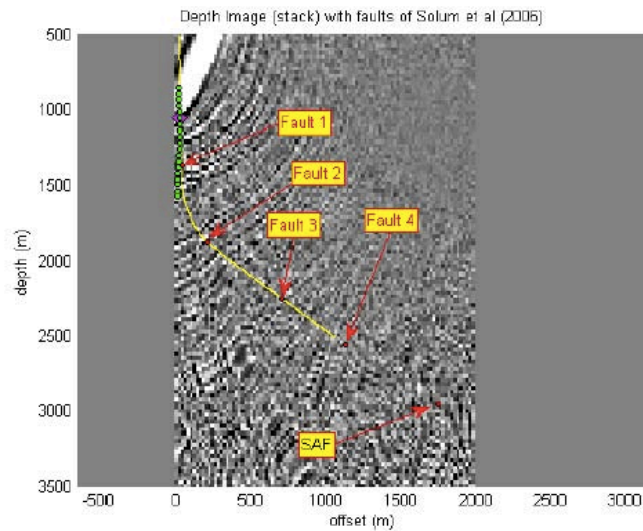


REVEALING A STRIKE-SLIP PLATE BOUNDARY: DRILL-BIT  
SEISMIC IMAGING OF THE SAN ANDREAS FAULT AT THE  
SAFOD SITE

by

Stewart Thomas Taylor

Department of Earth and Ocean Sciences  
Duke University



**Interferometric deconvolution of VSP data**  
*Stewart Taylor\** Duke University, and *Douglas E. Miller,*  
*Jakob B.U. Haldorsen, and Richard Coates,*  
*Schlumberger-Doll Research*

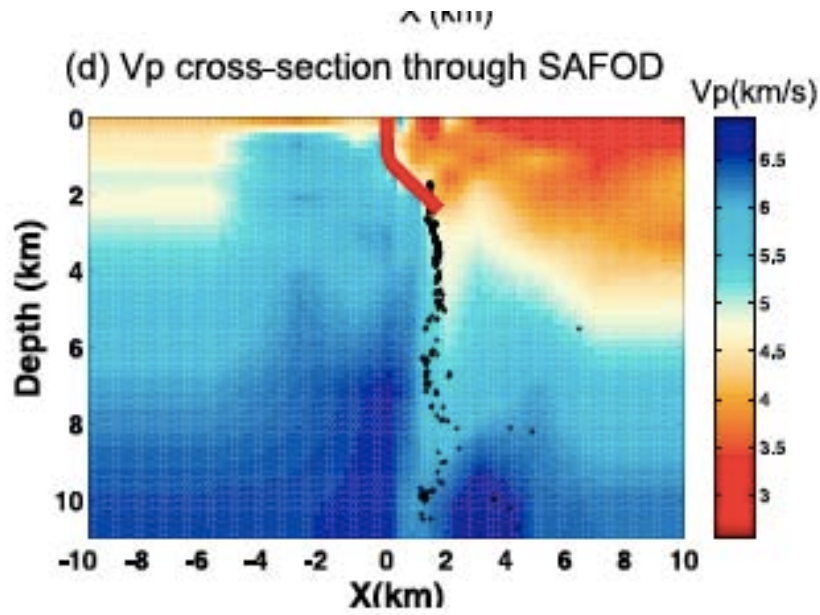


Figure 20: Satellite image of the SAFOD site. The location of the SAFOD drilling rig is marked by the yellow arrow. The location of the Buzzard Canyon Fault is indicated by the red arrow (Mike Rymer, USGS, personal communication, 2003). The trend of the Buzzard Canyon Fault is northwest and subparallel to the San Andreas Fault. Unmapped northwest trending faults associated with the Buzzard Canyon Fault are marked by dashed red lines which terminate at a northeast trending lineament going through the SAFOD site. Thayer (2006) mapped a high angle reverse fault transverse to the Buzzard Canyon fault at this location. We interpret the existence of a previously unmapped fault at the location of the solid red line based on passive seismic monitoring of microseismic activity. We refer to the fault at the solid red line as the SAFOD fault.

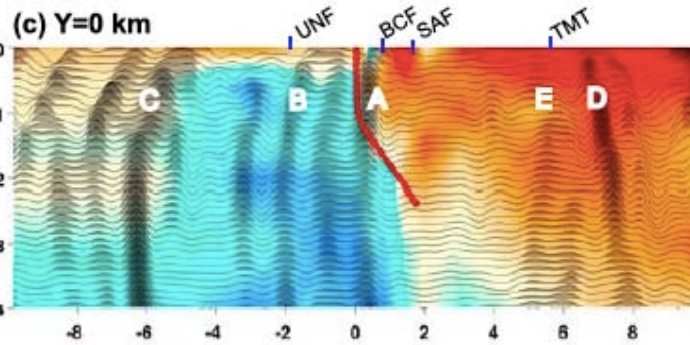
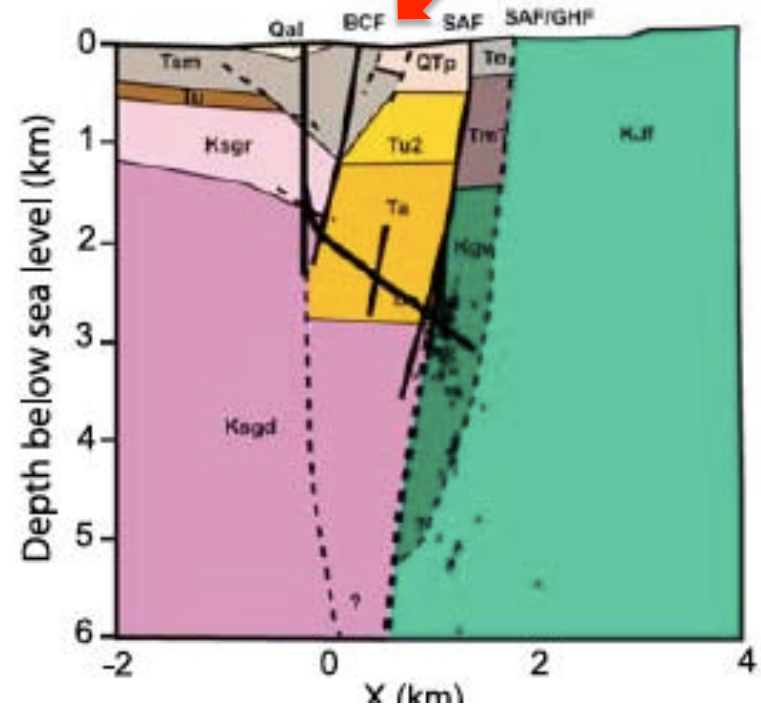
# Three-dimensional passive seismic waveform imaging around the SAFOD site, California, using the generalized Radon transform

Haijiang Zhang,<sup>1</sup> Ping Wang,<sup>1</sup> Robert D. van der Hilst,<sup>1</sup> M. Nafi Toksoz,<sup>1</sup> Clifford Thurber,<sup>2</sup> and Lupei Zhu<sup>3</sup>

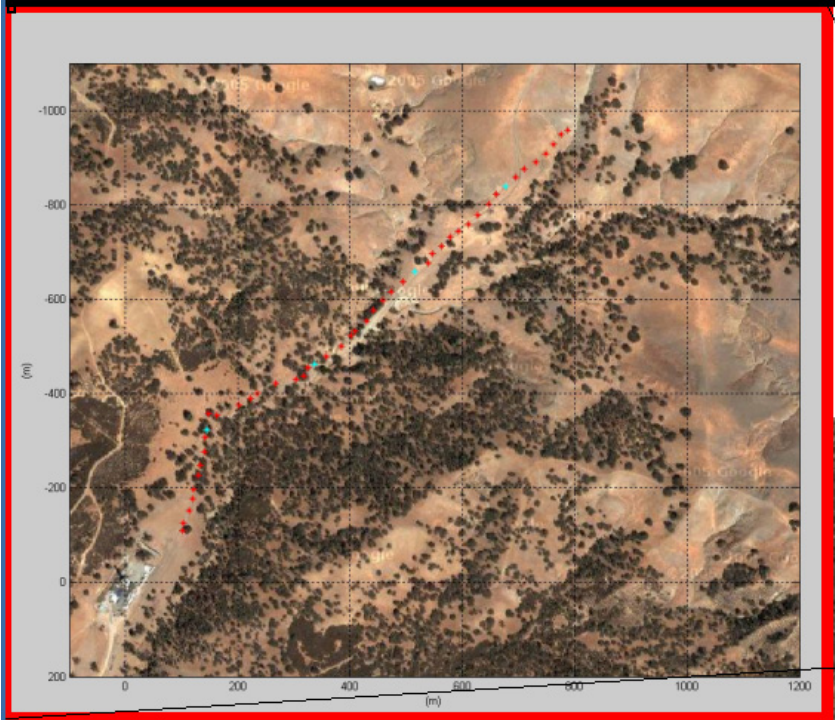
Received 11 August 2009; revised 30 October 2009; accepted 10 November 2009; published 9 December 2009.



(b) Geology cross-section through SAFOD

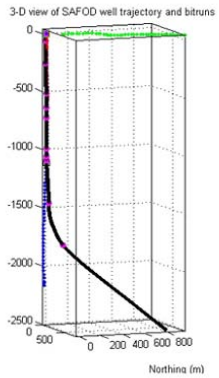


- 3 Component Borehole seismic array in pilot hole
- Short-spacing 3-component surface array



□

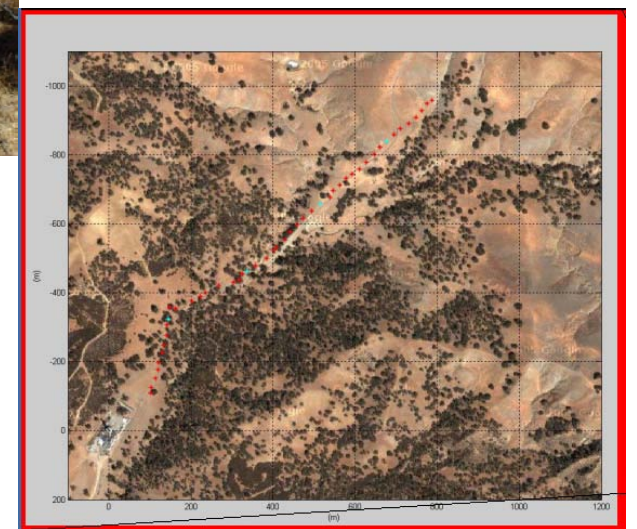
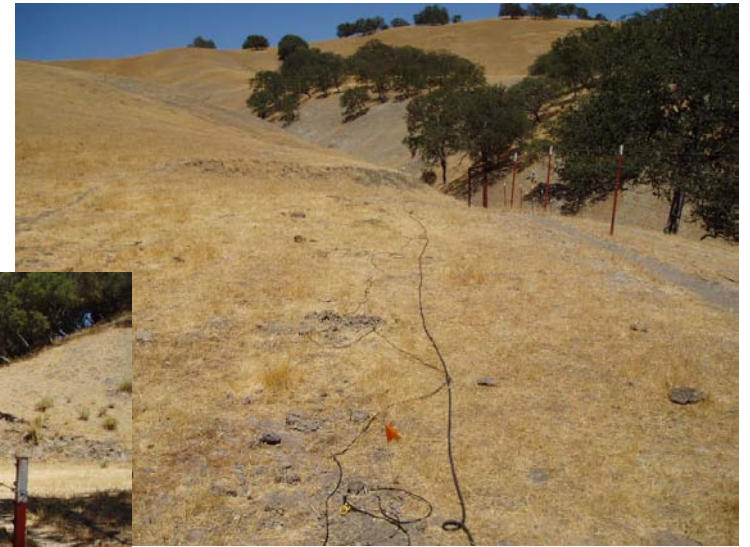
# Duke Data Set



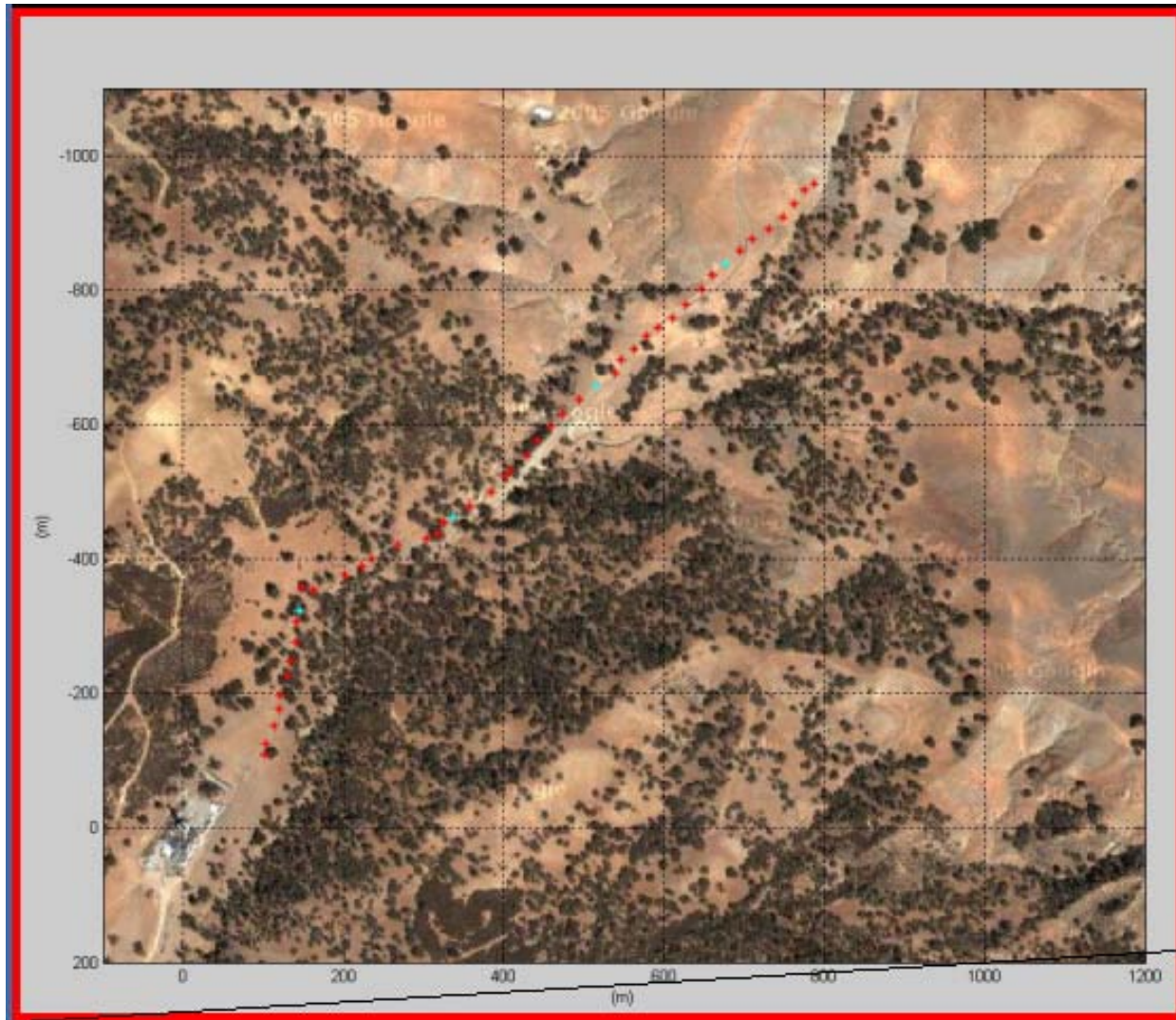
- 3 Component Borehole seismic array in pilot hole
- Short-spacing 3-component surface array



# Duke Data Set



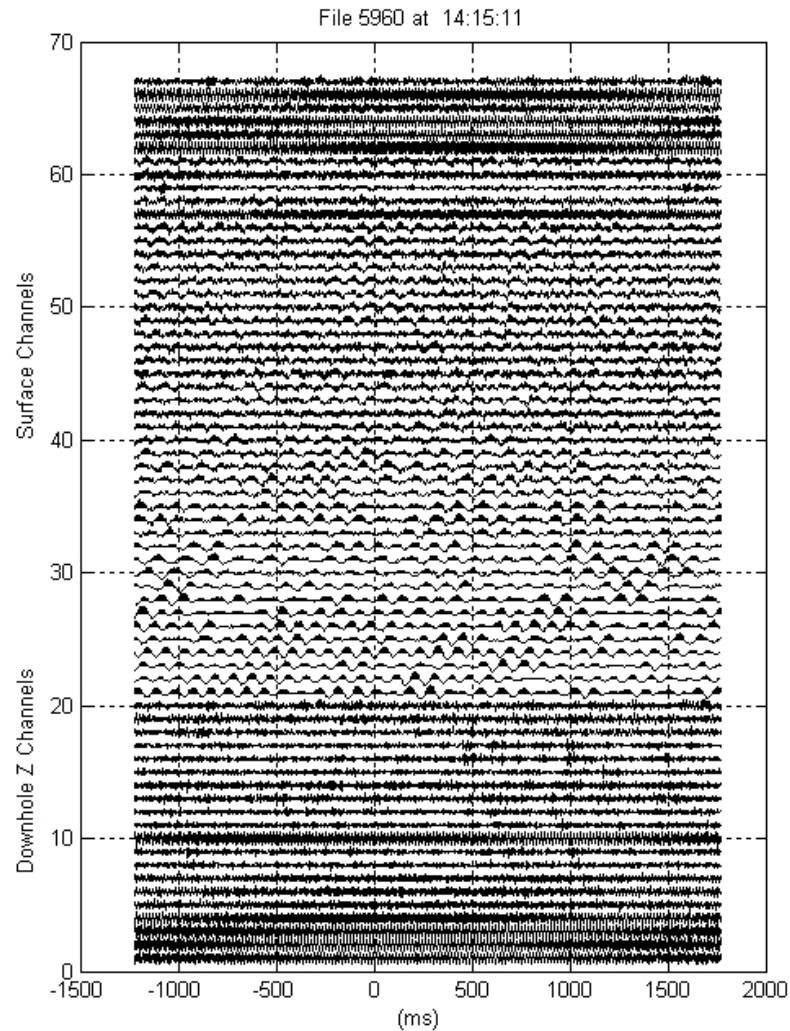
# Duke Data Set



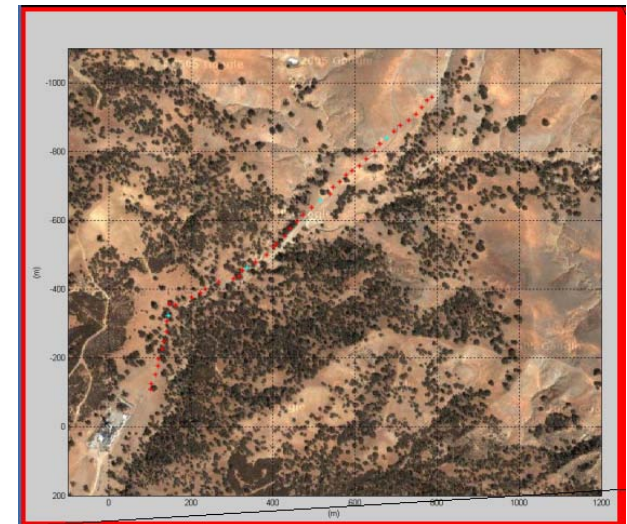
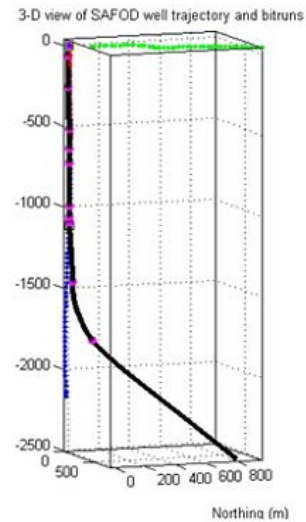
- C1:C19 Pilot Hole Z
- C20 Rig Accelerometer
- C21:C66 Surface Z
- C67 Rig Accelerometer



# Duke Data Set



- C1:C19 Pilot Hole Z
- C20 Rig Accelerometer
- C21:C66 Surface Z
- C67 Rig Accelerometer



# Outline

- SAFOD & the Duke/USGS Data set
- A Bit of Interferometry
- Simple Tomography with Earthquake Source Data

# What is Seismic Interferometry?

## ***Seismic interferometry—turning noise into signal***

*ANDREW CURTIS, University of Edinburgh, UK*

*PETER GERSTOFT, University of California at San Diego, USA*

*HARUO SATO, Tokoku University, Japan*

*ROEL SNIEDER, Colorado School of Mines, USA*

*KEES WAPENAAR, Delft University of Technology, The Netherlands*

**Definition of seismic interferometry.** The term *interferometry* generally refers to the study of interference phenomena between pairs of signals in order to obtain information from the differences between them. Seismic interferometry simply refers to the study of interference of seismic-related signals. The principal mathematical operation used to study this interference is crosscorrelation of pairs of signals, but one could equivalently consider convolution as the principal operation because crosscorrelation is simply convolution with the reverse of one of the two signals. The signals themselves may come from background-propagating waves or reverberations in the Earth, from earthquakes, from active artificial seismic sources, from laboratory sources, or from waveforms modeled on a computer—examples of using all of these data types will be given below.

- Operators built using data correlation
- So data-adaptive deconvolution is interferometry

# Old Wine for New Bottles

GEOPHYSICS, VOL. 60, NO. 4 (JULY-AUGUST 1995); P. 978-997, 19 FIGS., 3 TABLES.

## Walk-away VSP using drill noise as a source

Jaob B. U. Haldorsen\*, Douglas E. Miller‡, and John J. Walsh\*\*

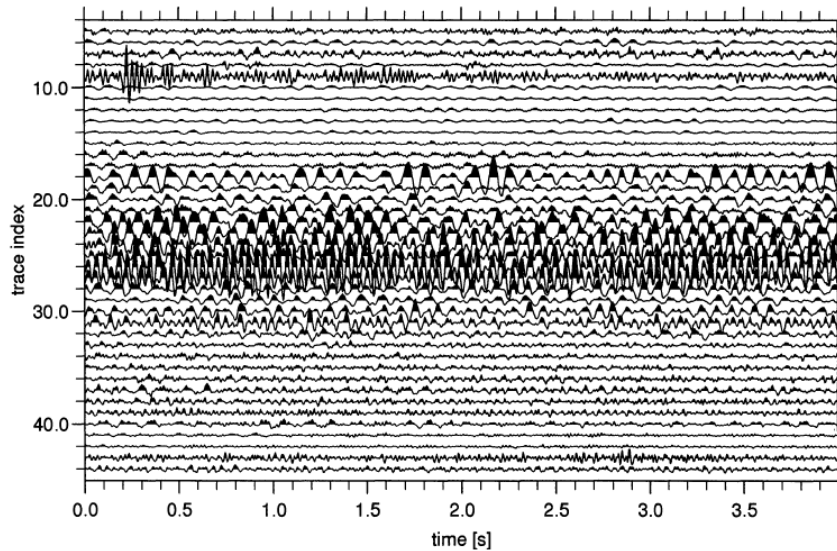


FIG. 3. A 4 s subrecord of raw drill-noise data. The rig site is located about 300 m away from the center of the line.

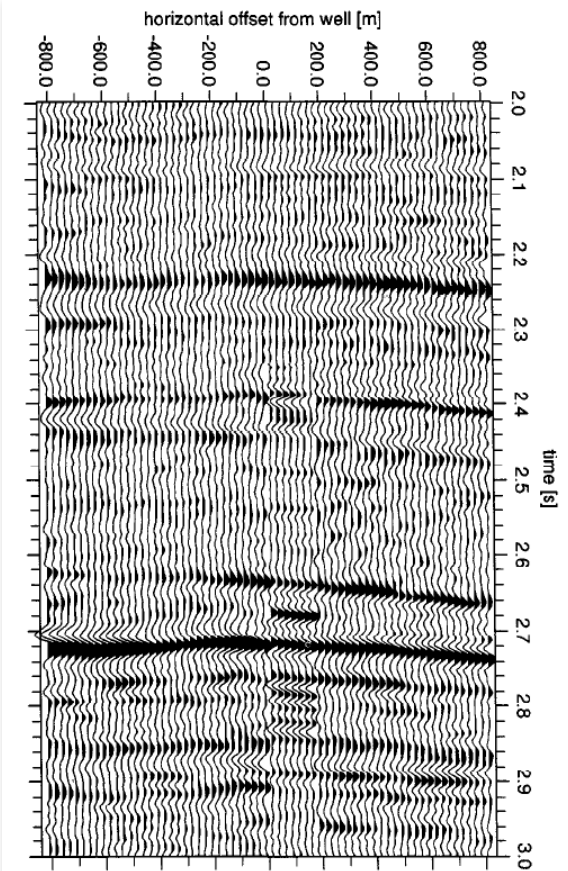


FIG. 17. The seismic image obtained from the optimally deconvolved drill-noise data.

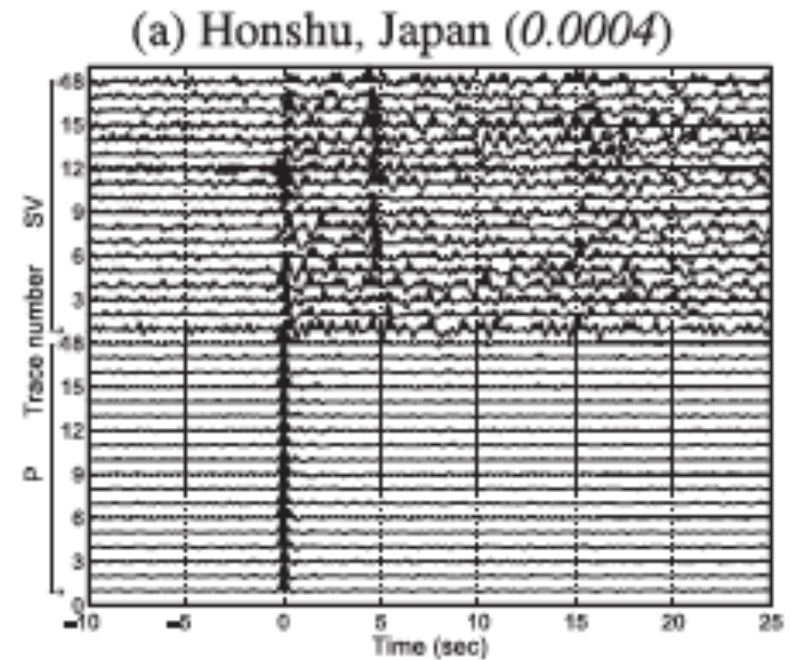
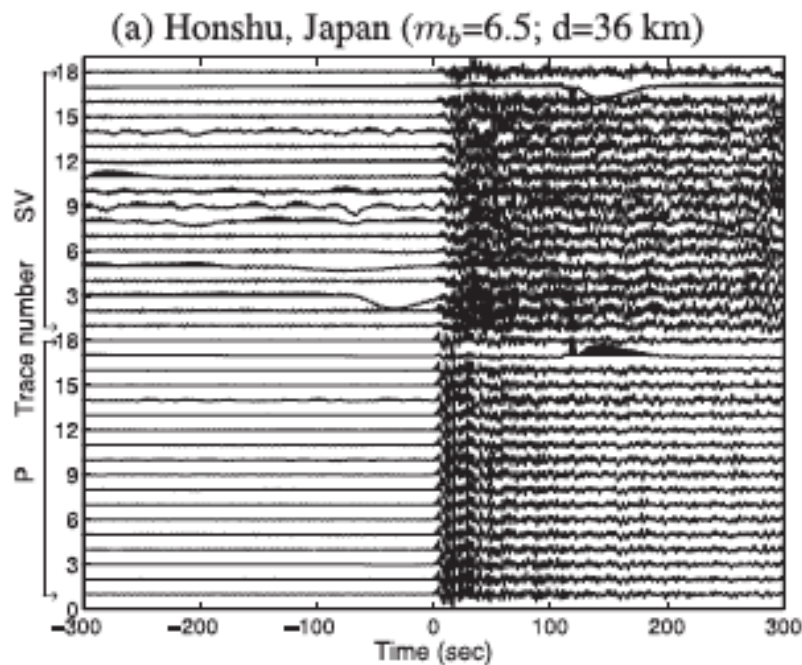
## Array-conditioned deconvolution of multiple-component teleseismic recordings

C.-W. Chen,<sup>1\*</sup> D. E. Miller,<sup>2</sup> H. A. Djikpesse,<sup>2</sup> J. B. U. Haldorsen<sup>2</sup> and S. Rondenay<sup>1</sup>

<sup>1</sup>*Department of Earth, Atmospheric and Planetary Sciences, Massachusetts Institute of Technology, Cambridge, MA 02139, USA*

*E-mail: cwchen@mit.edu*

<sup>2</sup>*Department of Mathematics and Modeling, Schlumberger-Doll Research, Cambridge, MA 02139, USA*



GEOPHYSICS, VOL. 59, NO. 10 (OCTOBER 1994); P.1500-1511, 9 FIGS., 2 TABLES.

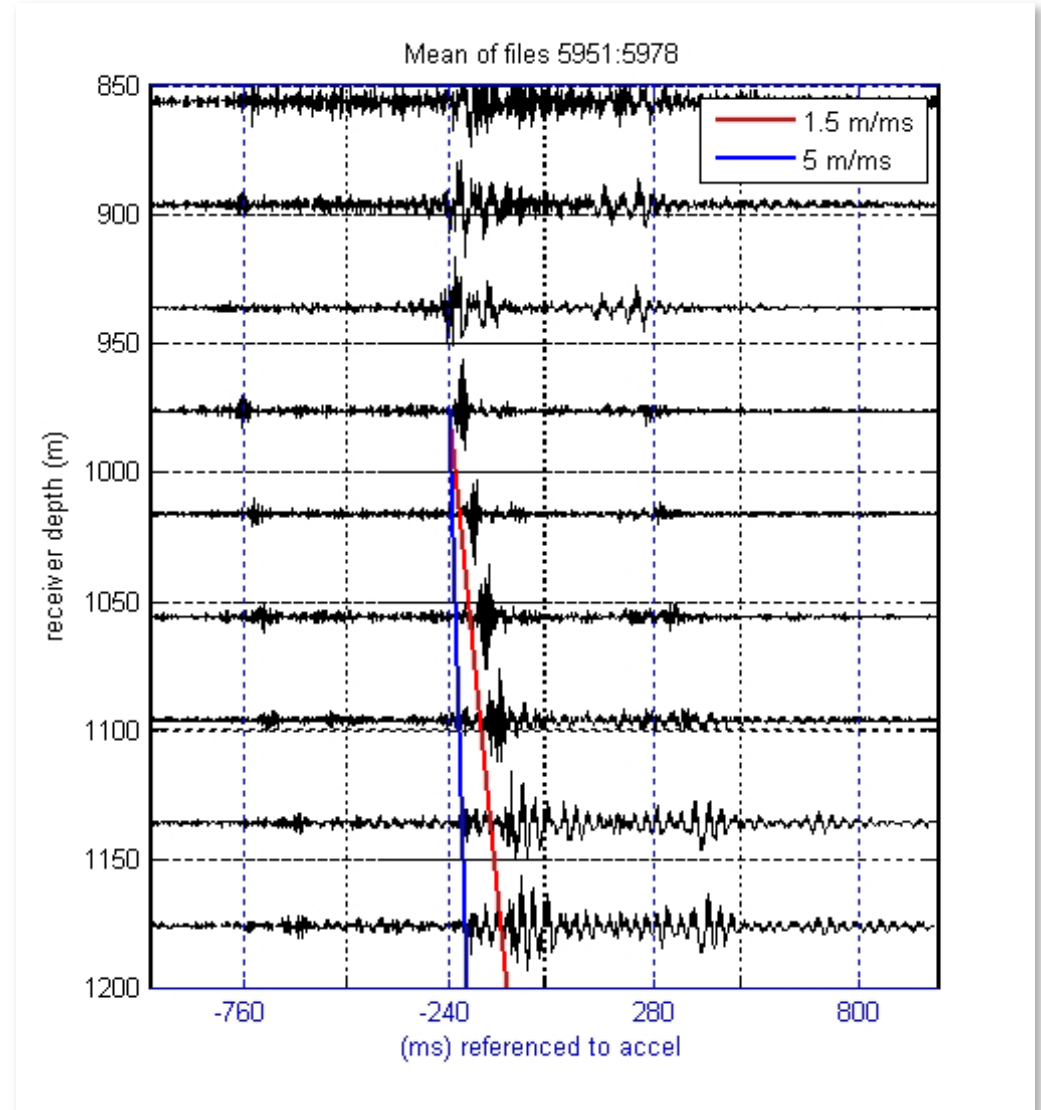
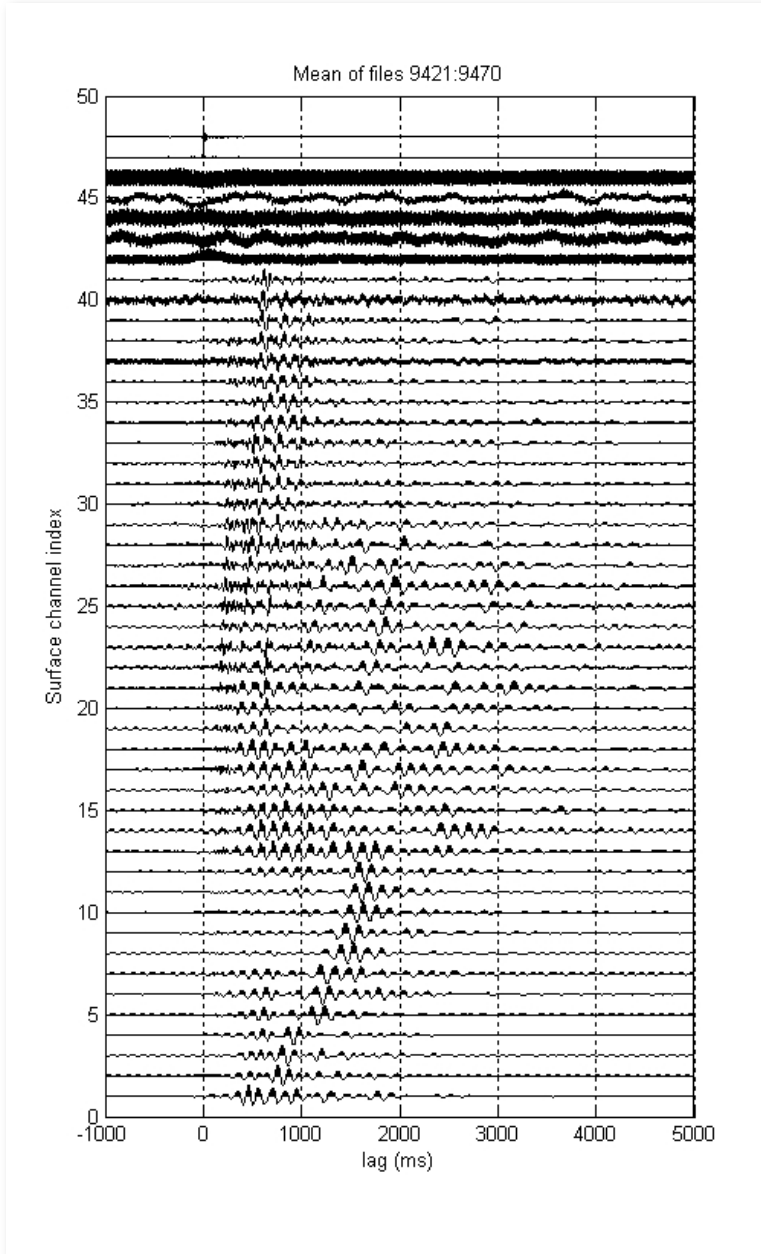
## Multichannel Wiener deconvolution of vertical seismic profiles

$$F(\omega) = \frac{\hat{f}^*(\omega)}{|\hat{f}(\omega)|^2 + E_N(\omega)}$$

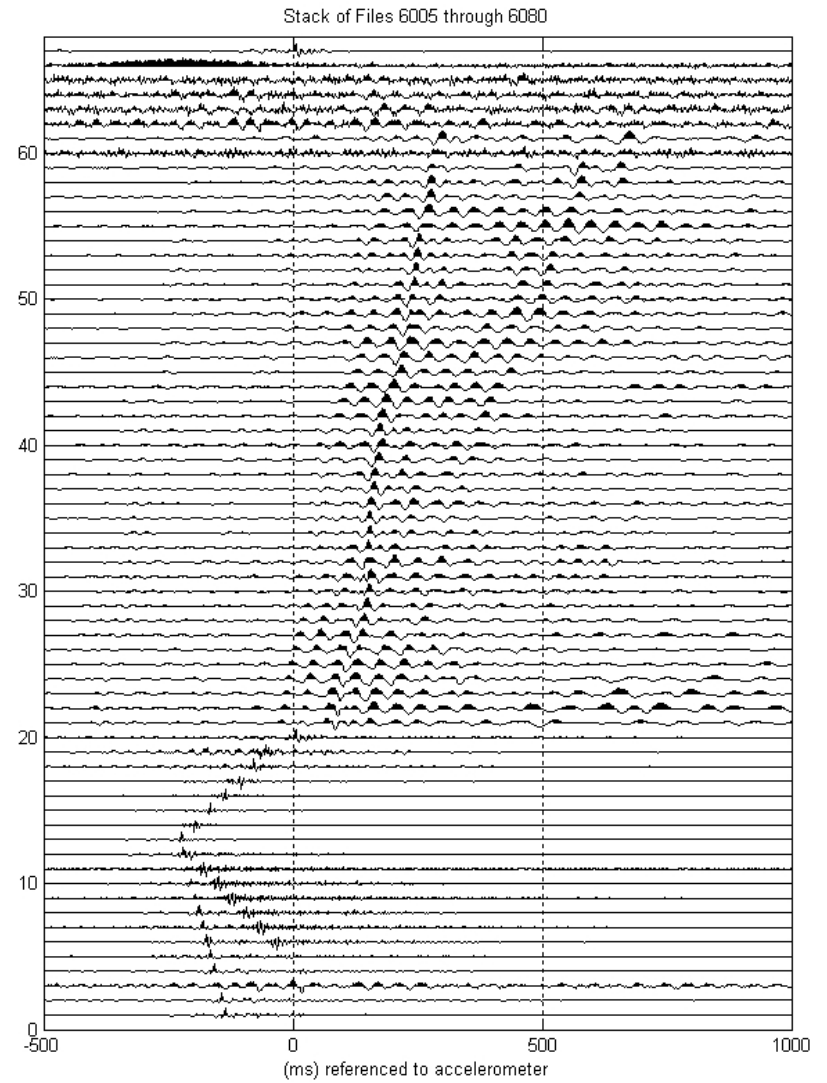
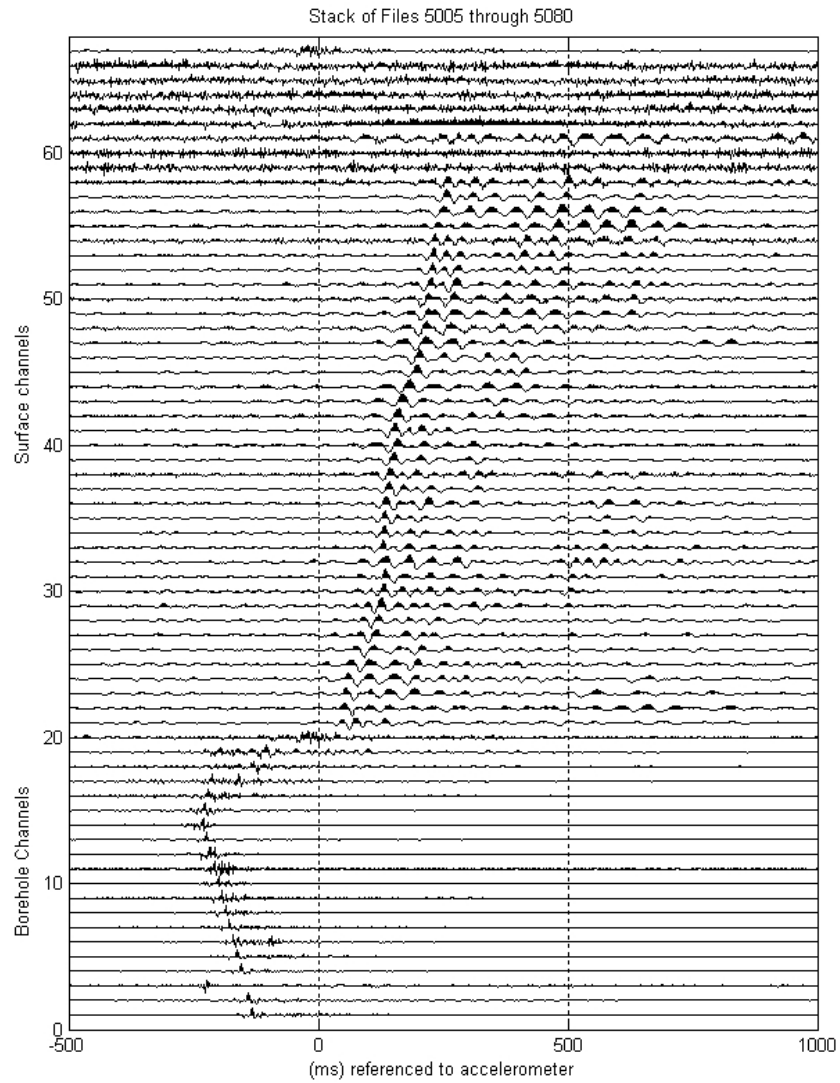
Jakob B.U. Haldorsen\*, Douglas E. Miller<sup>‡</sup>, and John J. Walsh\*\*

- Numerator is conjugate of estimated signal (including phase terms)
- If denominator is omitted (replaced by 1), operator becomes correlation with pilot. If  $E_N$  is estimated by a constant that's water-level decon.
- Array decon uses data total energy (and does not depend on phase).
- Solves  $F^*s = 1$

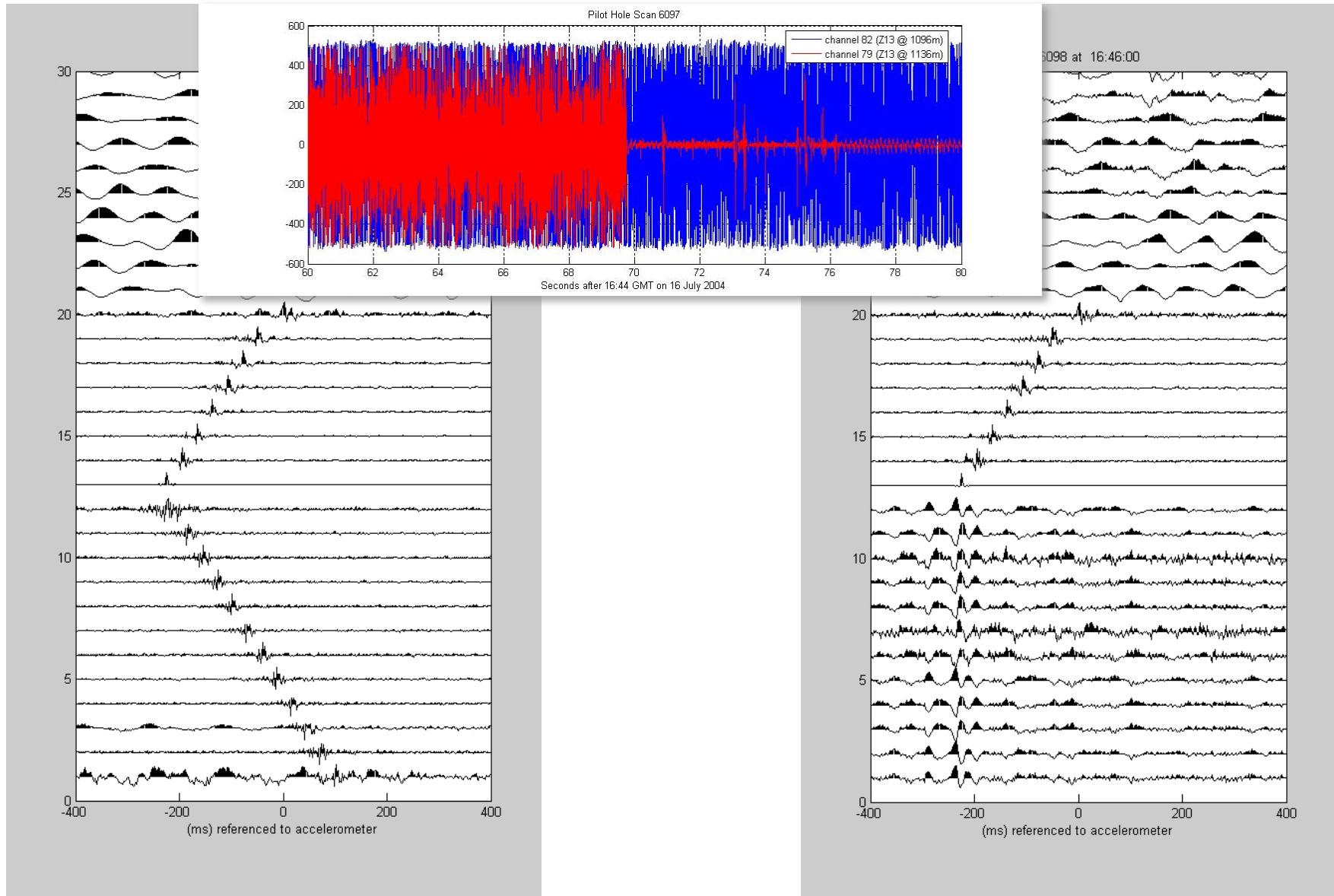
# First Results: Rig Accelerometer



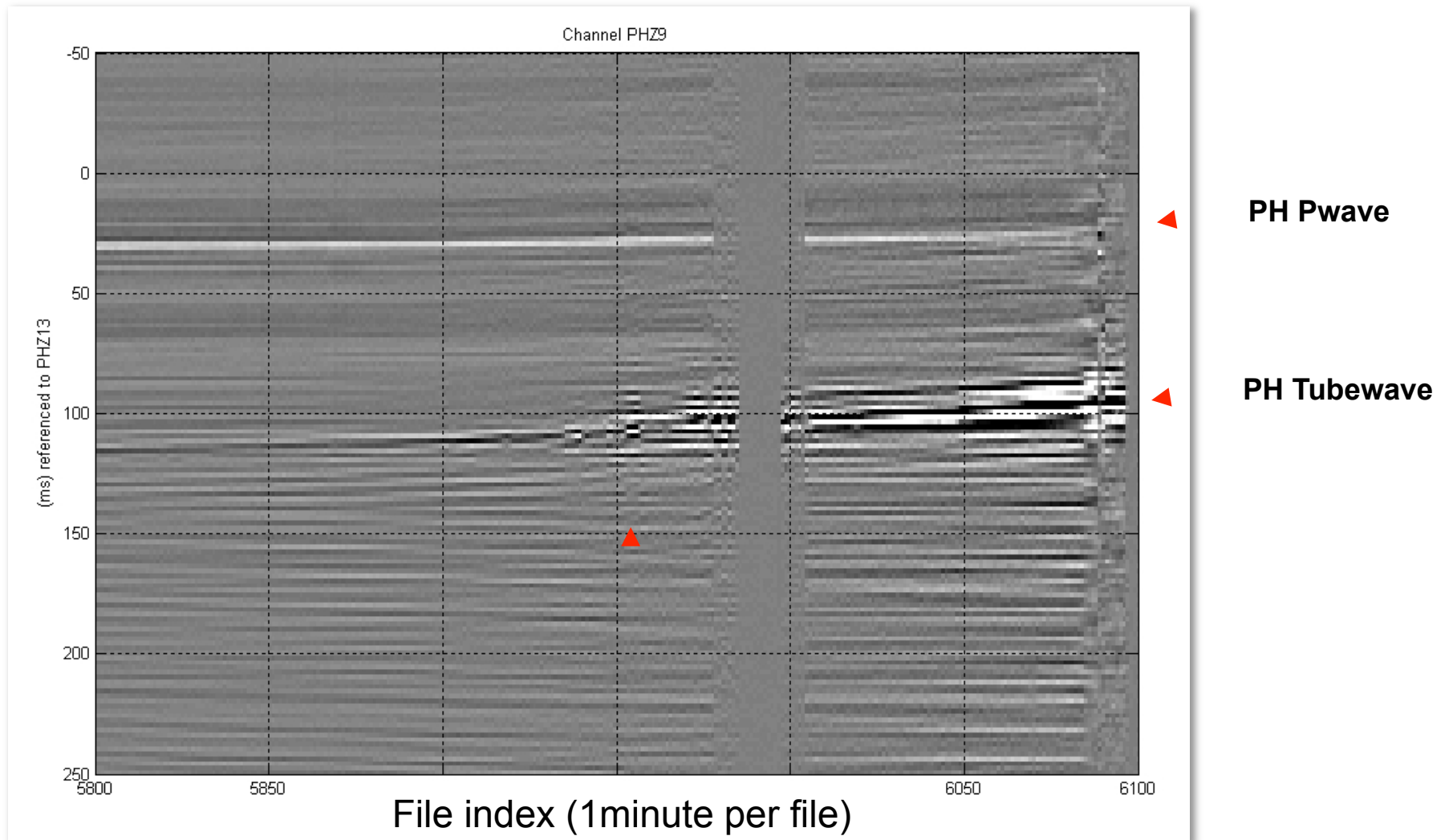
# Better Results: PHC13 as pilot



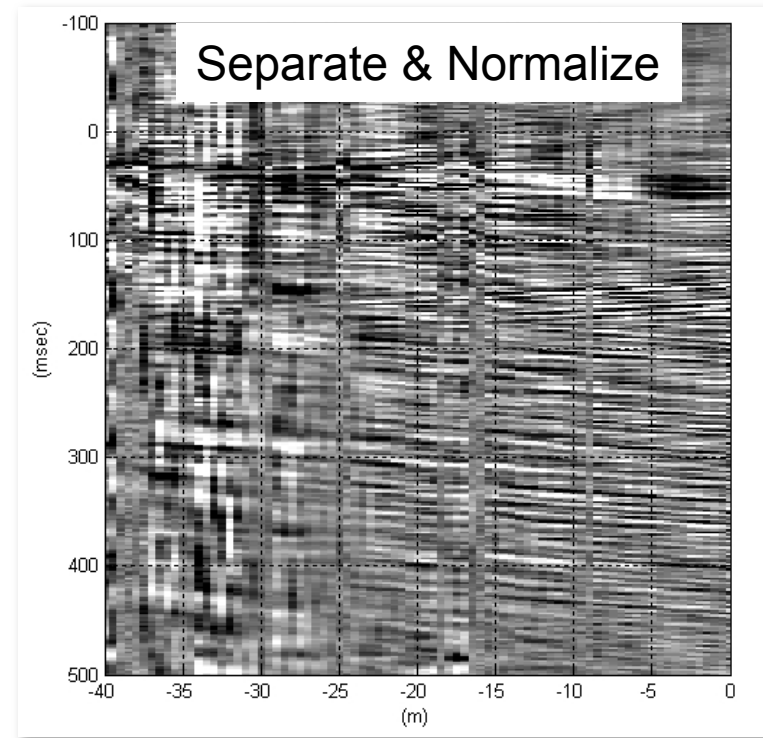
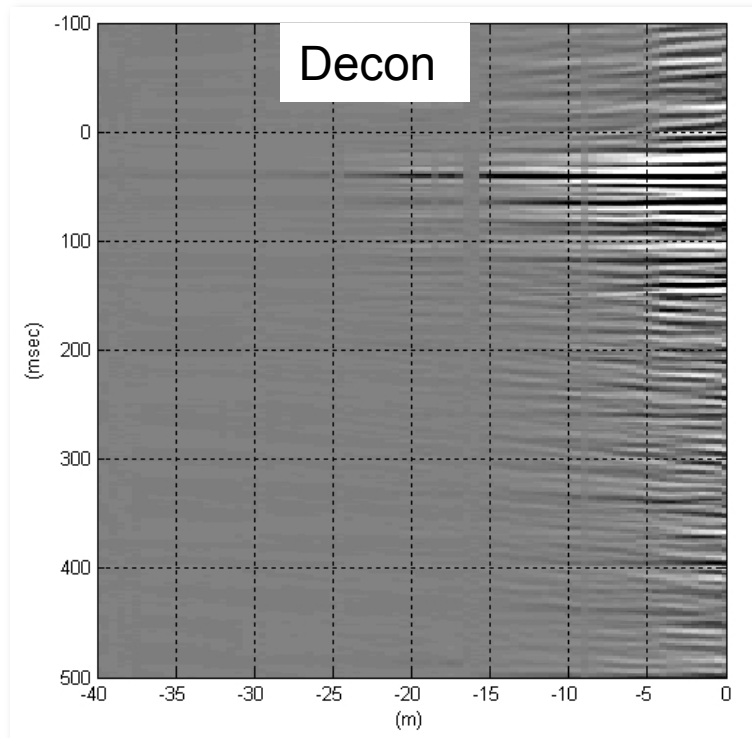
# 16 July 2004: An Unfortunate Encounter



# Channel 9Z at 1256m

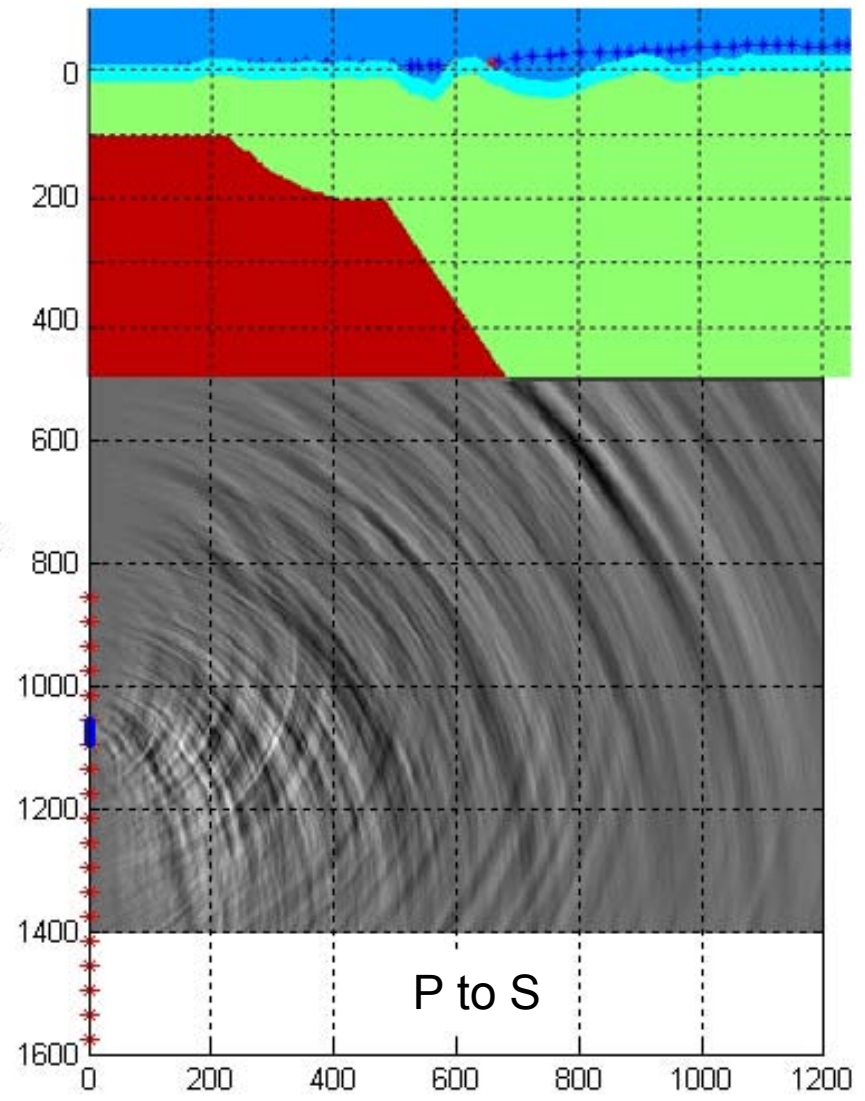
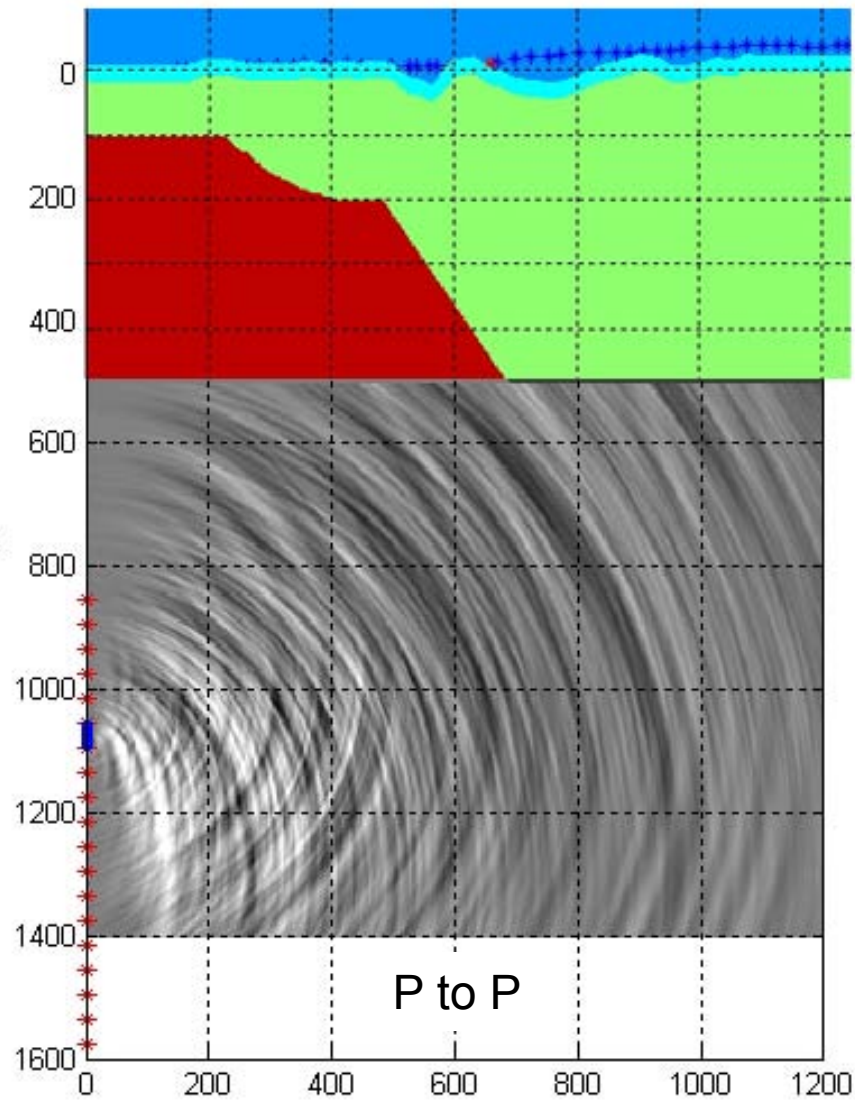


# Data for Imaging



- Aligned gladiator channels for pilot; all borehole channels for conditioning
- Bin-process common receiver gathers to remove direct arrival
- Normalize using tracewise rms noise estimate
- Migrate with homogeneous velocity model ( $V_p = 5.6$  km/sec,  $V_s = 3.2$  km/sec)

# Drillnoise Images



# Additional DNSP Images

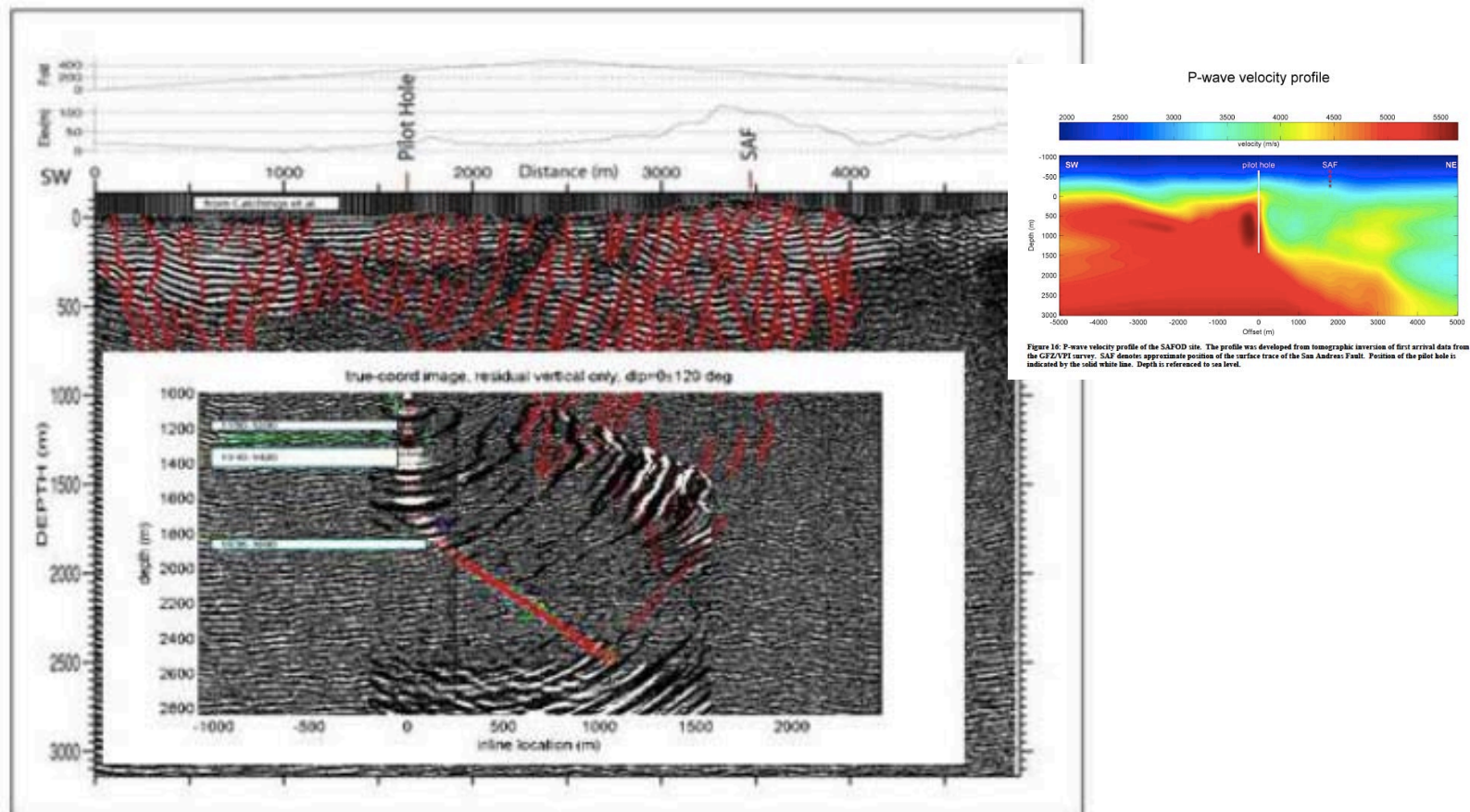


Figure 5-8: USGS PSINE profile and inset of drill bit seismic data. The inset shows the migrated drill bit seismic data and the path of the SAFOD well. Rectangles within the inset are locations of major shear zones as interpreted by Boness and Zoback (2004).

Made by Haldorsen & Taylor from surface data. From Stewart (2006)

# Additional DNSP Images

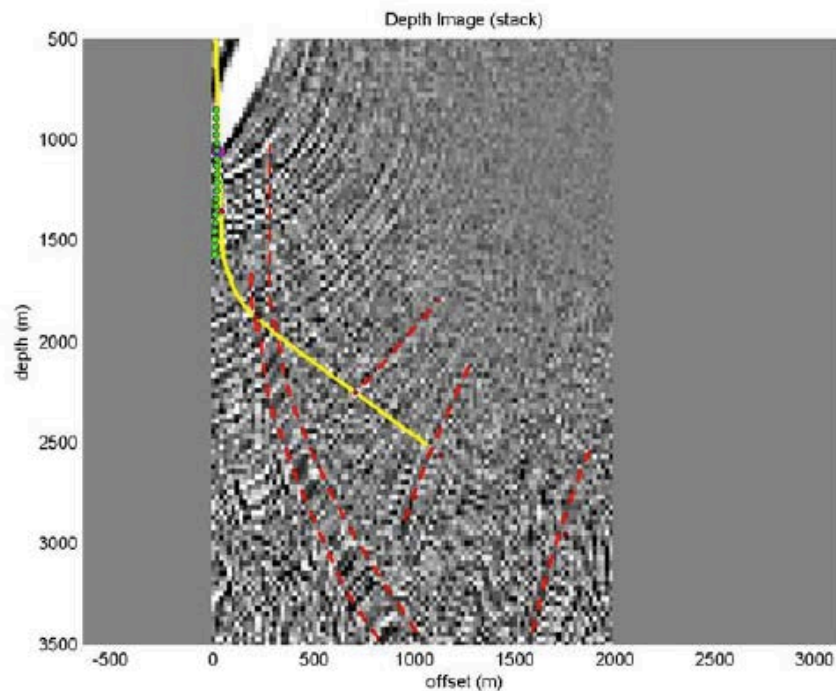


Figure 6-1: Depth image of the SAFOD site. This is the same image as Figure 5-10 but with faults interpreted using data from Solum et al (2006). The path of the wellbore is indicated by the yellow line with the position of the bit at the time of these recording indicated by the magenta diamond.

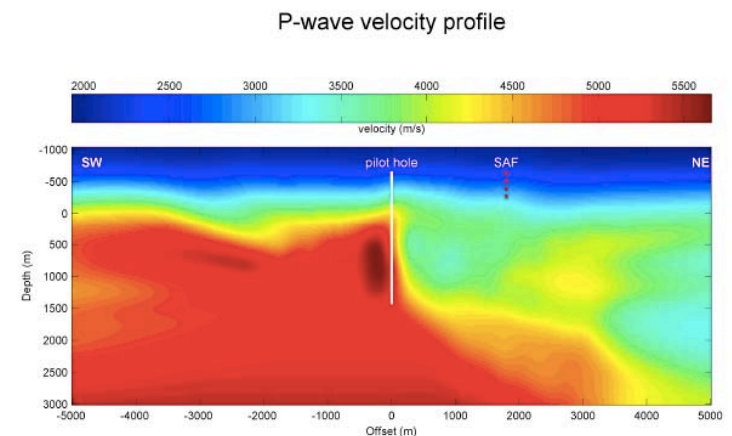


Figure 16: P-wave velocity profile of the SAFOD site. The profile was developed from tomographic inversion of first arrival data from the GFZ/VPI survey. SAF denotes approximate position of the surface trace of the San Andreas Fault. Position of the pilot hole is indicated by the solid white line. Depth is referenced to sea level.

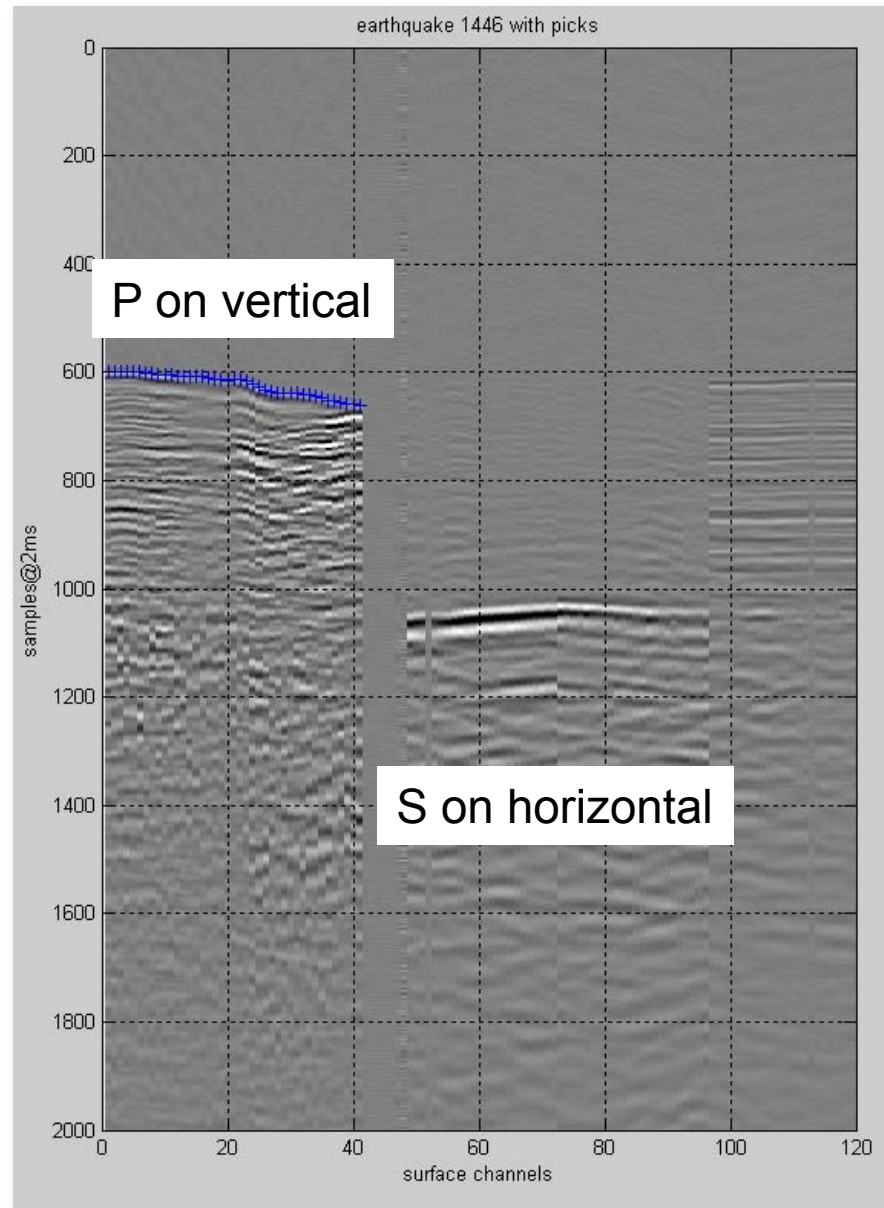
Made by Haldorsen & Taylor from combined surface & downhole data. From Stewart (2006)

# Outline

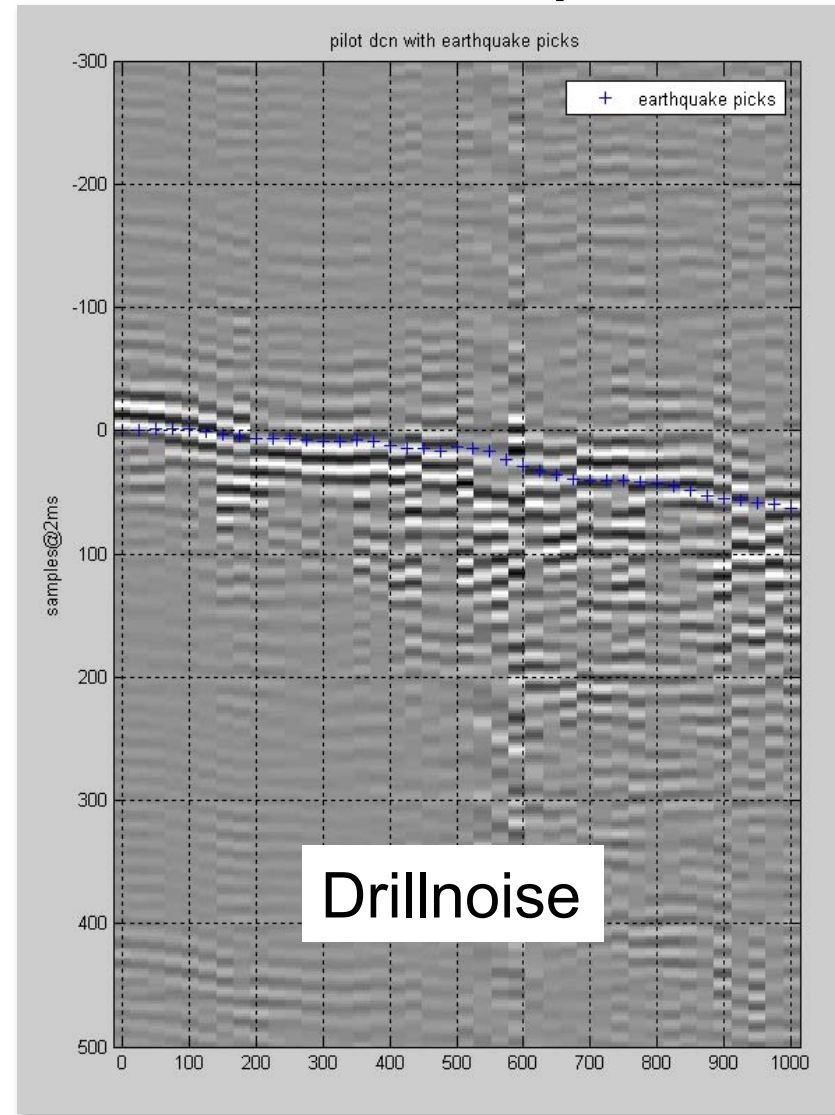
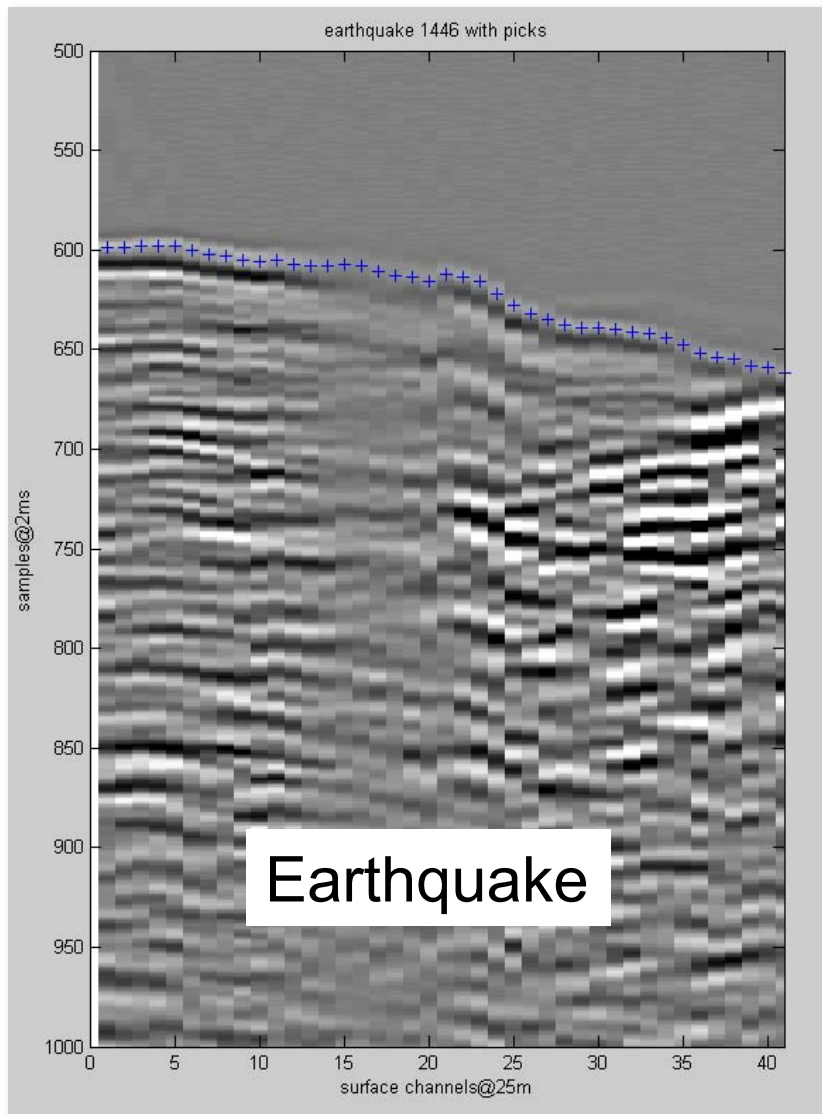
- SAFOD & the Duke/USGS Data set
- A Bit of Interferometry
- Simple Tomography with Earthquake Source Data



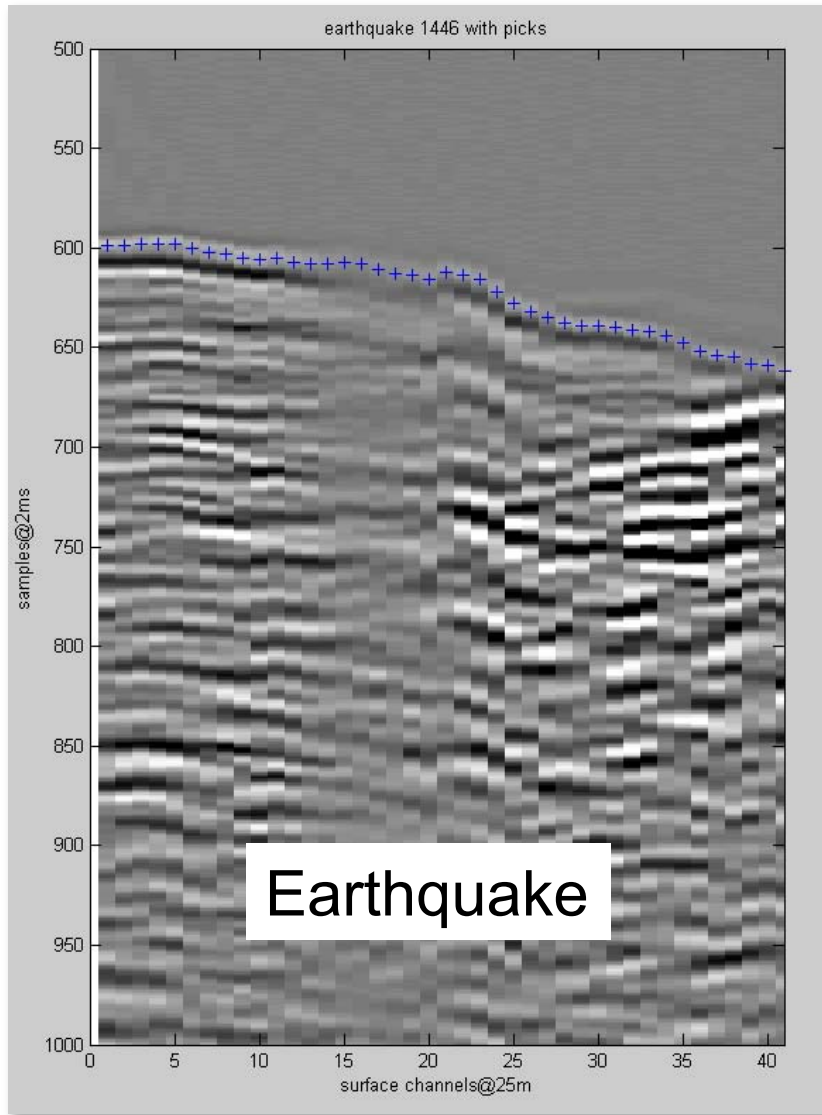
# Earthquake at about 7km



# Deconvolved Drillnoise with EQ Timepicks



# EQ Timepicks



P-wave velocity profile

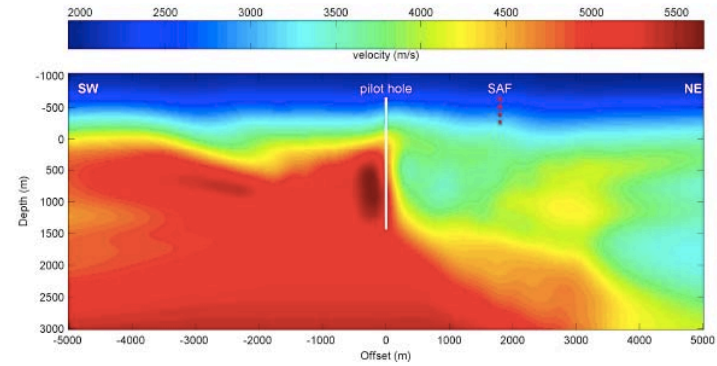
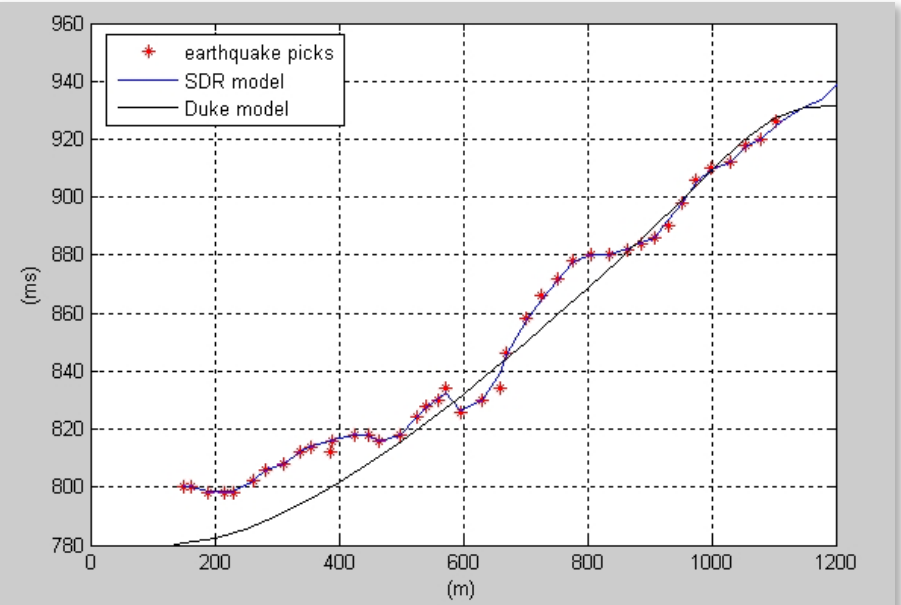
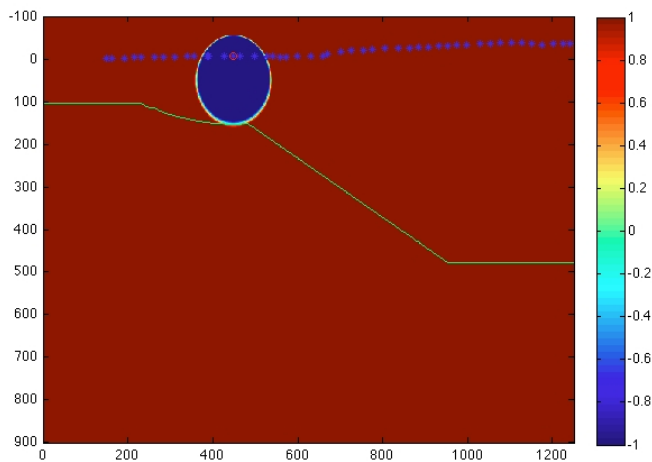
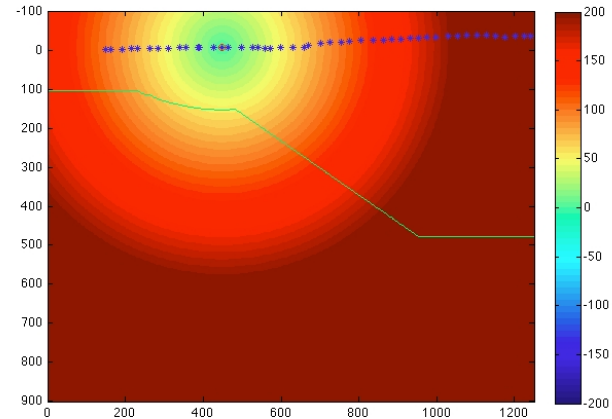
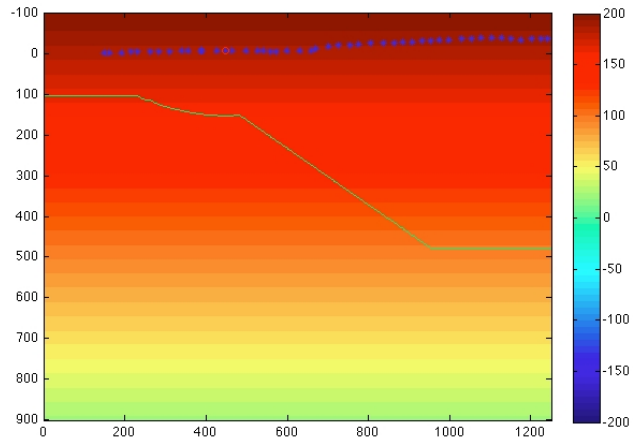


Figure 16: P-wave velocity profile of the SAFOD site. The profile was developed from tomographic inversion of first arrival data from the GEZ/VPI survey. SAF denotes approximate position of the surface trace of the San Andreas Fault. Position of the pilot hole is indicated by the solid white line. Depth is referenced to sea level.

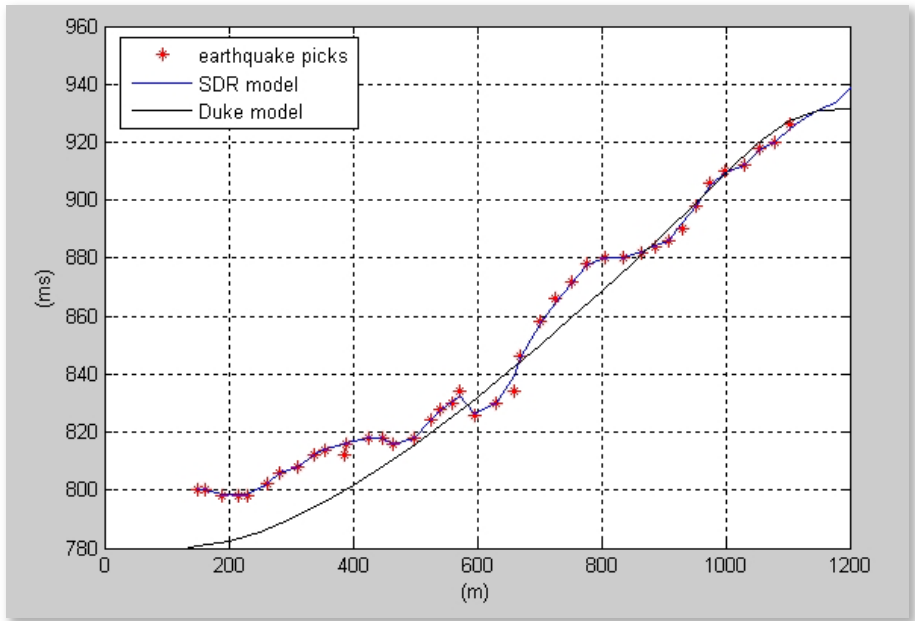
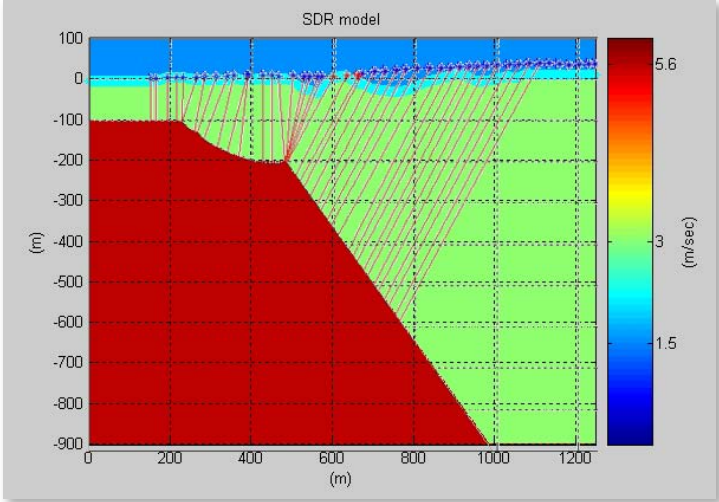
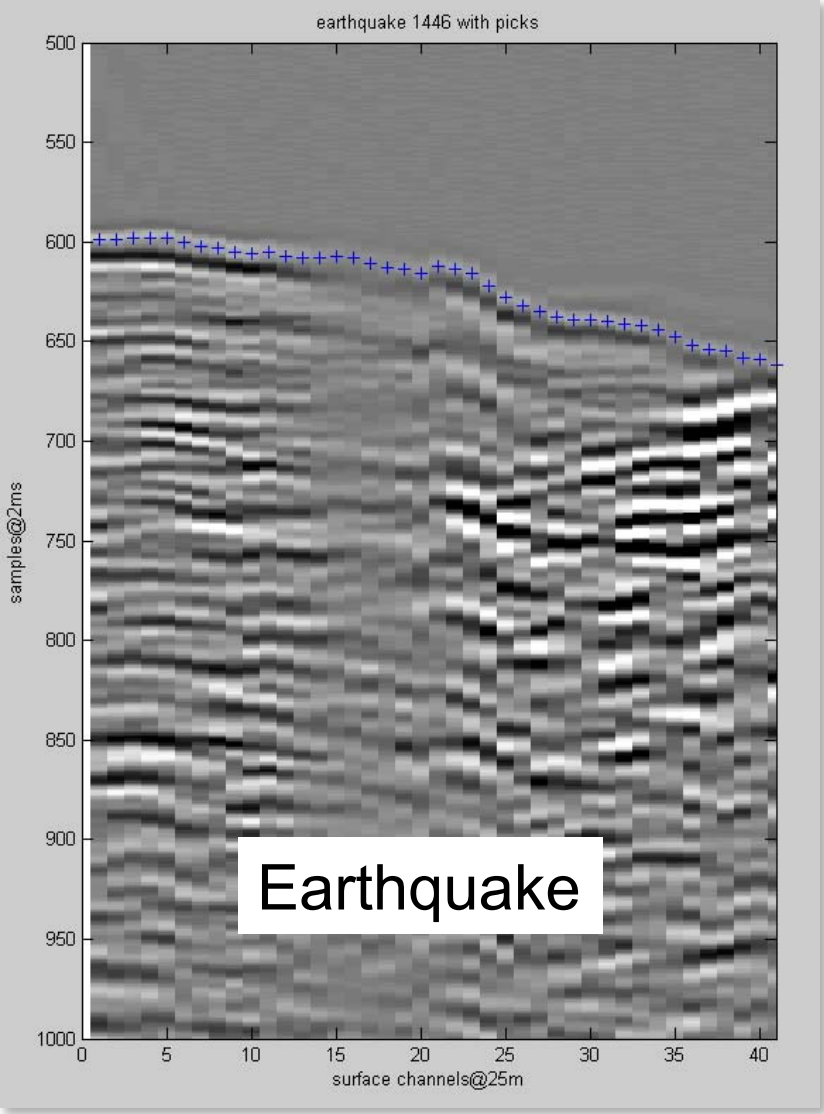


# Lensmaker's Tomography

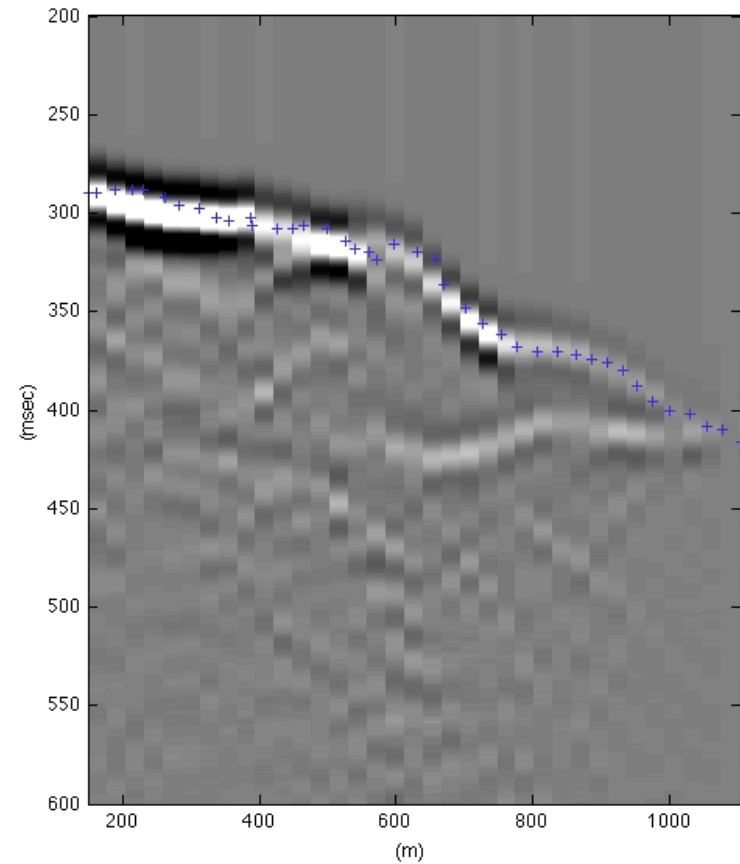
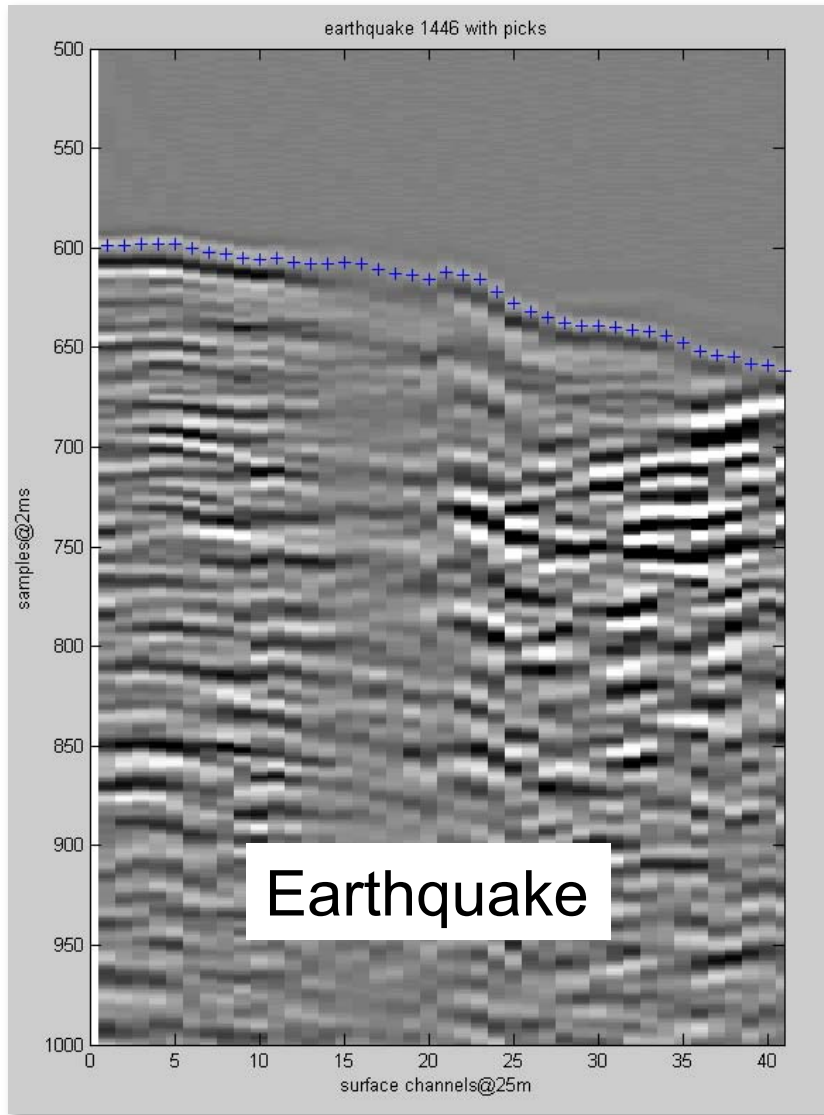


- $T_s$  = Traveltime from source in source medium
- $T_r$  = Traveltime from receiver in receiver medium
- Points where  $T_s + T_r < T_{meas}$  must be inside receiver medium

# Block Model to fit EQ Timepicks

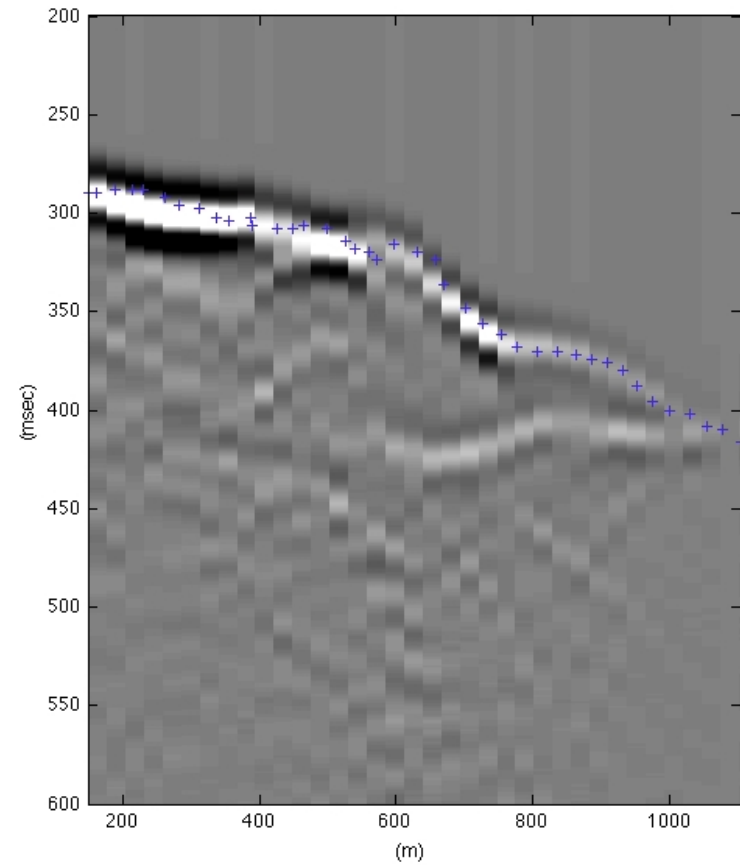
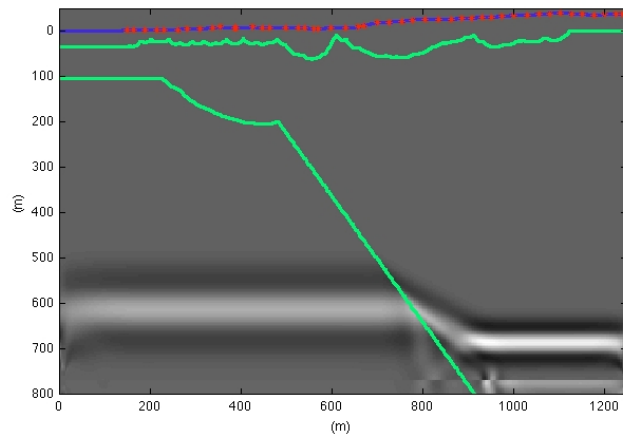
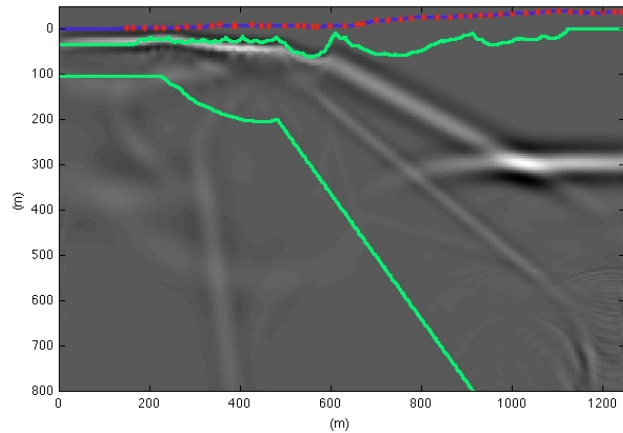


# Finite-Difference Synthetic



ERL-FD Model  
(thanks to Yang Zhang, et al)

# Finite-Difference Synthetic



ERL-FD Model

# Comments

- Array Decon looks like a robust & versatile tool.
- Lensmask tomography could be applied to more earthquake records
- The collision between main well & pilot hole was probably influenced by guiding in a plane of weakness associated with a transverse fault
- Thanks for your attention